The Mechanisms Involved in Seed Dormancy Alleviation by Hydrogen Cyanide Unravel the Role of Reactive Oxygen Species as Key Factors of Cellular Signaling during Germination[C][W]

Krystyna Oracz, Hayat El-Maarouf-Bouteau, Ilse Kranner, Renata Bogatek, Françoise Corbineau, and Christophe Bailly*

UPMC Univ Paris 06, Unité de Recherche 5, Germination et Dormance des Semences, Site d'Ivry, F–75005 Paris, France (K.O., H.E.-M.-B., F.C., C.B.); Department of Plant Physiology, Warsaw University of Life Sciences, 02–776 Warsaw, Poland (K.O., R.B.); and Seed Conservation Department, Royal Botanic Gardens, Wakehurst Place, West Sussex RH17 6TN, United Kingdom (I.K.)

The physiological dormancy of sunflower (*Helianthus annuus*) embryos can be overcome during dry storage (after-ripening) or by applying exogenous ethylene or hydrogen cyanide (HCN) during imbibition. The aim of this work was to provide a comprehensive model, based on oxidative signaling by reactive oxygen species (ROS), for explaining the cellular mode of action of HCN in dormancy alleviation. Beneficial HCN effect on germination of dormant embryos is associated with a marked increase in hydrogen peroxide and superoxide anion generation in the embryonic axes. It is mimicked by the ROS-generating compounds methylviologen and menadione but suppressed by ROS scavengers. This increase results from an inhibition of catalase and superoxide dismutase activities and also involves activation of NADPH oxidase. However, it is not related to lipid reserve degradation or gluconeogenesis and not associated with marked changes in the cellular redox status controlled by the glutathione/glutathione disulfide couple. The expression of genes related to ROS production (*NADPHox*, *POX*, *AO1*, and *AO2*) and signaling (*MAPK6*, *Ser/ThrPK*, *CaM*, and *PTP*) is differentially affected by dormancy alleviation either during after-ripening or by HCN treatment, and the effect of cyanide on gene expression is likely to be mediated by ROS. It is also demonstrated that HCN and ROS both activate similarly *ERF1*, a component of the ethylene signaling pathway. We propose that ROS play a key role in the control of sunflower seed germination and are second messengers of cyanide in seed dormancy release.

The effect of cyanide (potassium cyanide [KCN] or hydrogen cyanide [HCN]) in releasing seed dormancy has been demonstrated many years ago, mainly for cereals (Roberts, 1973; Roberts and Smith, 1977; Côme et al., 1988) and to a lesser extent for members of other plant families, such as the Asteraceae (Esashi et al., 1979) and Rosaceae (Bogatek and Lewak, 1988). However, at the cellular and molecular level, the mechanisms by which HCN breaks dormancy remain unclear. Unraveling the HCN-dependent mechanisms of dormancy release is challenging because HCN inhibits a major metabolic event, respiration, and also various enzymes involved in other biochemical pathways and is therefore likely to alter cell metabolism dramatically. Oracz et al. (2007, 2008) recently proposed that a short-term treatment (3 h) with gaseous cyanide could act as a signal involved in the alleviation of embryo dormancy in sunflower seeds. Interestingly, this dormancy breaking effect of cyanide was not attributable to the inhibition of respiration or the stimulation of the oxidative pentose phosphate pathway, as suggested by different authors (Roberts and Smith, 1977; Côme and Corbineau, 1990).

A novel role was assigned to this compound since it was demonstrated that cyanide triggered an irreversible and specific protein carbonylation that was associated with dormancy alleviation (Oracz et al., 2007). Carbonylation can result from oxidative attack and corresponds to the introduction of carbon monoxide into a molecule (Berlett and Stadtman, 1997). Hence, the dormancy breaking effect of cyanide could be a consequence of reactive oxygen species (ROS) accumulation. This hypothesis receives support from an increasing number of publications that provide evidence for a key role for ROS in seed germination and dormancy alleviation (for review, see Bailly et al., 2008; El-Maarouf-Bouteau and Bailly, 2008), although the precise mechanisms by which ROS affect seed dormancy status and germination remain to be elucidated. Moreover, it has also been suggested that ROS

* Corresponding author; e-mail christophe.bailly@upmc.fr.

The author responsible for distribution of materials integral to the findings presented in this article in accordance with the policy described in the Instructions for Authors (www.plantphysiol.org) is: Christophe Bailly (christophe.bailly@upmc.fr).

[C] Some figures in this article are displayed in color online but in black and white in the print edition.

[W] The online version of this article contains Web-only data.

www.plantphysiol.org/cgi/doi/10.1104/pp.109.138107

might play a key role in hormone signaling pathways (Kwak et al., 2006). A complex network of plant hormones, including abscisic acid (ABA), GAs, ethylene, auxin, brassinosteroids, and jasmonates, controls seed dormancy and germination (Finkelstein et al., 2008), but the cross talk between ROS and hormones is still poorly understood. Interestingly, in dormant sunflower (*Helianthus annuus*) seeds, whose dormancy is released by ethylene (Corbineau et al., 1990), cyanide triggered the expression of the transcription factor Ethylene Response Factor1 (ERF1), thus suggesting a cross talk between ethylene and cyanide pathways (Oracz et al., 2008). However, it has not been investigated so far whether ROS signal transduction might be involved in this cross talk.

Therefore, this work was undertaken to determine whether ROS could mediate HCN signal in seed dormancy alleviation and, more widely, to assess their putative role in the control of seed germination. The production of ROS was measured and localized in embryonic axes of sunflower seeds in response to HCN treatment and during germination. To determine whether ROS are involved in dormancy alleviation, ROS-producing and -scavenging chemicals were applied during seed imbibition and their effects on seed dormancy status assessed. As the maintenance of the cellular ROS homeostasis requires a fine-tuned balance between ROS production and scavenging (Miller et al., 2008), we investigated the effects of cyanide on the activities of the ROS-processing enzymes, catalase (CAT), superoxide dismutase (SOD), and glutathione reductase (GR), and on the concentrations of glutathione (GSH) and glutathione disulphide (GSSG) in the embryonic axes. GSH is the major intracellular thiol antioxidant and also participates in the control of the cellular redox status (Foyer and Noctor, 2005; Kranner et al., 2006). The potential effect of HCN on ROS-producing enzymes was assessed using the NADPH-oxidase inhibitor, diphenyleneiodonium (DPI), and by studying the expression of NADPH oxidase (*NADPHox*), peroxidase (*POX*), and amine oxidase (*AO1* and *AO2*) genes. NADPH oxidase is a plasma membrane-bound enzyme that catalyzes the production of $O_2^{\bullet -}$ by the reduction of ground state oxygen using NADPH as an electron donor (Lamb and Dixon, 1997). Cell wall peroxidases may form hydrogen peroxide (H_2O_2) in the presence of a reductant. Their role in ROS production has been investigated mainly with regard to biotic stress (Bolwell and Wojtaszek, 1997; Bindschedler et al., 2006). Apoplastic amine oxidases produce H_2O_2 from amine oxidation, and they have been proposed to mediate lignification and response to biotic and abiotic stresses (Laurenzi et al., 1999; Rea et al., 2004; Cona et al., 2006). Alternatively, if dormancy alleviation by HCN involves ROS, signaling via HCN and ROS might then have some downstream elements in common. The expression of some major genes involved in ROS signal transduction (Desikan et al., 2001) was therefore investigated in response to HCN treatment. Genes studied were *MAPK6*, *Ser/ThrPK*, *CaM*, and *PTP*. Xing et al. (2008) proposed that MAPK6 is a pivotal mediator in cellular stress signaling. MAPK6 belongs to the group of mitogen-activated protein kinases (MAPKs) and is activated by various stresses, such as cold, drought, wounding, or oxidative stress (Jonak et al., 2002). Ser/Thr protein kinases (Ser/Thr PKs) also participate in ROS signal transduction to AtMPK6 (Rentel et al., 2004). Both calmodulin (CaM) and protein Tyr phosphatase (PTP) are two components of the H_2O_2 signaling pathway (Desikan et al., 2001). For example, the cross talk between Ca^{2+}-CaM and H_2O_2 seems to play a key role in ABA signaling (Hu et al., 2007). PTPs can be reversibly inactivated under oxidative conditions and are involved in regulating cellular responses to redox changes (Dixon et al., 2005). They also down-regulate ABA signaling during seed germination in Arabidopsis (*Arabidopsis thaliana*; Quettier et al., 2006). Since gluconeogenesis is a putative source of ROS (Graham, 2008), the effect of HCN on the embryonic axis content of soluble sugars was also assessed. Finally, we also aimed to determine whether the dormancy breaking effect of HCN on gene expression was specific for this compound or could be relate to ROS accumulation. Therefore, we investigated the effect of the ROS-generating compound methylviologen (MV) on the expression of the above-mentioned genes and on the expression of the major genes involved in ethylene signaling, namely, *ETR1*, *ETR2*, *ERS1*, *CTR1*, and *ERF1*. Indeed, in a previous study (Oracz et al., 2007), it was shown that there existed a cross talk between ethylene and HCN pathways.

The results presented in this study allow us to present a comprehensive view of the mechanisms of HCN-dependent dormancy release in sunflower seeds, in which ROS signaling plays a major role. More generally, this data set also proposes a role for ROS as key players in the regulation of seed dormancy and germination.

RESULTS

Cyanide and ROS-Generating Compounds Alleviate Dormancy, and the Effect of Cyanide Is Partially Prevented by the NADPH Oxidase Inhibitor DPI

Only approximately 20% of the dormant sunflower embryos germinated at 10°C when the nondormant ones germinated easily within 4 d (Fig. 1A). Treatment of dormant embryos with gaseous HCN for 3 h alleviated dormancy (Fig. 1A). Ninety percent of HCN-treated embryos germinated after 5 d at 10°C, a temperature that prevents their germination on water, the time to obtain 50% germination being similar to that of nondormant embryos (2.6–2.8 d). Treatment of dormant embryos for 3 h with 1 mM MV or menadione (MN), two ROS-generating compounds (Calderbank and Slade, 1976; Thor et al., 1982), also allowed embryos to fully germinate at 10°C within 6 and 10 d,

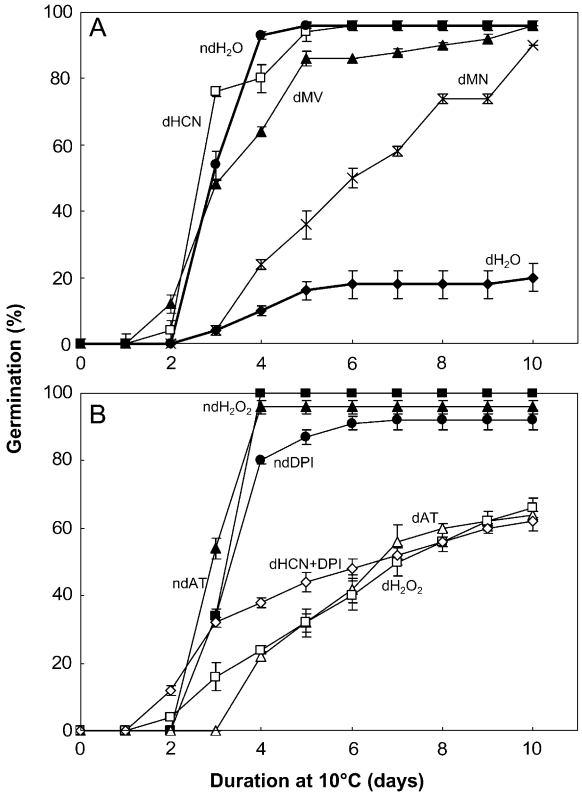

Figure 1. Germination of sunflower embryos from the same seed lot at 10°C in the dark. A, Dormant embryos (dH_2O) and after-ripened nondormant embryos (ndH_2O) on water, dormant embryos treated with 0.1 mM MV (dMV), 1 mM MN (dMN), and 2.24% gaseous HCN (dHCN). B, Dormant embryos treated by HCN and DPI combined (0.1 mM dHCN + DPI), H_2O_2 (0.5 mM dH_2O_2), and AT (1 mM dAT) and nondormant embryos germinated on 0.1 mM DPI (ndDPI), 0.5 mM H_2O_2 (ndH_2O_2), and 1 mM AT (ndAT). HCN, MV, and MN treatment were carried out for 3 h before transferring the embryos to wet cotton wool at 10°C. DPI, H_2O_2, and AT were applied continuously. Data are means of three replicates ± SD.

respectively (Fig. 1A). Treatment of dormant embryos with H_2O_2 or aminotriazole (AT), an inhibitor of CAT (Amory et al., 1992), also had a dormancy-breaking effect, although this promoting effect was less pronounced; 60% of H_2O_2- or AT-treated embryos germinated within 10 d at 10°C (Fig. 1B). In contrast, when dormant embryos were treated with HCN in the presence of DPI, an inhibitor of NADPH oxidase, the dormancy alleviation by HCN was partly reduced, and only 60% of embryos germinated after 10 d (Fig. 1B). DPI, AT, and H_2O_2 had no significant effect on the germination of nondormant embryos (Fig. 1B).

Cyanide Treatment Is Associated with ROS Production

To get further insights into the mechanisms of HCN-dependent dormancy alleviation, H_2O_2 and $O_2^{\bullet-}$ contents were measured in dry embryonic axes and upon imbibition at 10°C in the presence or absence of HCN and MV. Extending the data of Oracz et al. (2007), seed after-ripening was associated with the accumulation of H_2O_2 and $O_2^{\bullet-}$ (Table I). When imbibed at 10°C, axis of nondormant seeds contained more H_2O_2 and $O_2^{\bullet-}$ than those of dormant seeds after 3 and 24 h (Table I). At 24 h, H_2O_2 and $O_2^{\bullet-}$ accumulation were approximately 30% and 70% higher in nondormant than in dormant axes, respectively (Table I). HCN treatment was associated with a marked increase in H_2O_2 in both dormant and nondormant axes. At 24 h, H_2O_2 reached approximately 4.2 nmol g dry weight^{-1} in HCN-treated axes, whereas it was close to 2.5 nmol g dry weight^{-1} in control nontreated dormant axes imbibed with water only. Conversely, HCN did not change $O_2^{\bullet-}$ production in either dormant or nondormant axes (Table I). At last, MV treatment was always associated with an increase in H_2O_2 and $O_2^{\bullet-}$ production, to a level very close to the one reached in the presence of HCN.

To establish a stronger link between ROS and HCN, we applied the HCN treatment in the presence of a general free radical scavenger, sodium benzoate (Hung and Kao, 2004), a specific superoxide scavenger, 1,2-dihydroxy-benzene-3,5-disulphonic acid (Tiron; Wise and Naylor, 1987), or H_2O_2 scavengers, dimethylthiourea (DMTU; Levine et al., 1994), ascorbate, and GSH (Noctor and Foyer, 1998). These compounds did not modify significantly the germination of nondormant embryos, suggesting that they were not toxic at the concentration used (1 mM), but they inhibited slightly the germination of dormant embryos, with the exception of DMTU, which had almost no effect (Table II). The beneficial effect of HCN on germination of dormant embryos was strongly repressed in the presence of all the scavengers tested (Table II).

ROS were visualized in embryonic axes by confocal microscopy using 5-(and-6)-chloromethyl-2′,7′-dichlorofluorescein diacetate (DCFH-DA), producing fluorescent spots within the cells at the sites of ROS formation (Fig. 2). Figure 2A shows a view of sunflower embryo, with axis and cotyledon. Confocal sections were taken at the tip of the axis, as shown in Figure 2B. Toluidine blue staining shows that the axis consists of longitudinal rows of cells, and Figure 2C provides a schematic representation of the cellular territories of the radicle tip. After 24 h of imbibitions, fluorescence markedly developed in nondormant axes or HCN-treated dormant axes (Fig. 2, E and F) but was much weaker in dormant axes (Fig. 2D). Confocal microscopy revealed that ROS strongly accumulated close to the radicle tip, i.e. in root cap and lateral cap cells from germinating axes (Fig. 2, E and F). Fluorescence was also visible in cortex cells and in vascular tissues (Fig. 2, E and F). In dormant axes, fluorescence only appeared in the outer layers of cells of the root cap and was almost not detectable in the internal cell layers (Fig. 2D).

To determine whether cyanide could alter the in vivo activity of SOD, CAT, and GR, their activity was determined in vitro in the presence of various concen-

Table I. *ROS production in embryonic axes during imbibition*

H_2O_2 and superoxide ($O_2^{\bullet -}$) production in embryonic axes isolated from dormant (d) and after-ripened, nondormant (nd) sunflower embryos before imbibition (dry) and from embryos that were imbibed on water for 24 h at 10°C (H_2O), or treated for 3 h with 0.1 mM MV (MV) or with gaseous cyanide (HCN) and then transferred for 21 h on water at 10°C. Values are means of five replicates ± SD. DW, Dry weight.

Treatment	Duration of Imbibition	H_2O_2		$O_2^{\cdot -}$	
		d	nd	d	nd
	h	*nmol g DW^{-1}*		*nmol g DW^{-1}*	
No	0 (dry)	1.51 ± 0.21	2.10 ± 0.04	0.62 ± 0.03	0.91 ± 0.06
H_2O	3	2.12 ± 0.13	2.96 ± 0.09	0.63 ± 0.01	0.98 ± 0.05
HCN	3	2.81 ± 0.12	4.22 ± 0.2	0.70 ± 0.06	1.01 ± 0.06
MV	3	2.73 ± 0.11	3.11 ± 0.15	0.70 ± 0.04	0.99 ± 0.06
H_2O	24	2.50 ± 0.19	3.26 ± 0.17	0.61 ± 0.05	1.10 ± 0.06
HCN	24	4.25 ± 0.35	5.05 ± 0.11	0.67 ± 0.05	1.28 ± 0.06
MV	24	4.51 ± 0.17	5.44 ± 0.22	0.69 ± 0.03	1.20 ± 0.02

trations of KCN. This revealed a strong inhibitory effect of KCN on CAT and SOD activities, which decreased by 50% at KCN concentrations of 30 or 500 μM, respectively, while GR activity was not affected at any concentration tested (Supplemental Fig. S1).

Dormant and nondormant axes contained similar GSH and GSSG contents, indicating that seed afterripening was not associated with major changes in GSH redox state (Supplemental Table S1). Upon imbibition GSSG contents fell by 82% to 83%, both in dormant and nondormant axes, while GSH remained almost unchanged in nondormant axes but decreased by 14% in dormant ones. Compared to imbibition in water alone, HCN treatment did not significantly affect the GSH content of the embryonic axes but increased their GSSG content by 68% in dormant seeds and 31% in nondormant seeds and correspondingly, changed the GSH/GSSG ratio from 22.3 to 13.6, respectively (Supplemental Table S1).

Since gluconeogenesis may also lead to H_2O_2 production (Graham, 2008), we also measured the changes in soluble sugar content during the cyanide treatment of dormant embryonic axes (Table III). Suc was the major soluble sugar found in dry dormant axes, and its content was similar to the one found in nondormant axes (data not shown). Seed imbibition was associated with a progressive decrease in Suc, Fru, Glc, and raffinose content of dormant embryonic axes, and this trend was not modified by the HCN treatment (Table III). After 24 h of imbibition, hexoses (Glc and Fru) became undetectable in HCN-treated dormant axes.

Comparison of HCN and MV Effects on Gene Expression

In this study, we considered that one expression pattern differed significantly from another one when relative level of gene expression increased or decreased at least 2-fold. Supplemental Figure S2 shows the relative transcript levels, expressed as a function of the one determined in axes of dry dormant embryos, of some genes involved in ROS production (*HaNADPHox*, *HaPOX*, *HaAO1*, and *HaAO2*) and signaling (*HaSerThrPK*, *HaMAPK6*, *HaPTP*, and *HaCaM*) and in ethylene perception (*HaETR1*, *HaETR2*, *HaERS1*, *HaCTR1*, and *HaERF1*). The expression of ethylene signaling genes has already been studied by Oracz et al. (2008), but the effect of MV on this gene expression was carried out here to discriminate between a specific or ROS-mediated effect of HCN on their expression. According to our criteria, only the expression patterns of *HaPOX*, and very markedly that of *HaCaM*, were lower when embryos were treated by both HCN and MV (Supplemental Fig. S2). Preimbibition treatment of embryos with HCN resulted in a decrease in *HaAO2* but not in *HaAO1* expression (Supplemental Fig. S2). As previously shown, only the expression of *HaERF1* expression was markedly activated by HCN (Oracz et al., 2008; Supplemental Fig. S2). MV activated specifically the expression of *HaETR2* (Fig. 3) and dramatically the one of *HaERF1* (Supplemental Fig. S2).

Table II. *Effect of ROS scavengers on germination of embryos treated by HCN*

HCN treatment was carried out for 3 h before transferring the embryos to wet cotton wool at 10°C. ROS scavengers were applied continuously and their concentrations were 1 mM. Data are means of three replicates ± SD. SB, Sodium benzoate; ASA, ascorbic acid.

Treatment	Germination (%) after 7 d at 10°C of:	
	Dormant Embryos	Nondormant Embryos
Water	18 ± 4	96 ± 4
HCN	96 ± 3	97 ± 4
Tiron	13 ± 5	100 ± 0
HCN + Tiron	24 ± 2	–
SB	10 ± 3	98 ± 1
HCN + SB	27 ± 3	–
DMTU	17 ± 2	99 ± 1
HCN + DMTU	35 ± 4	–
ASA	11 ± 3	100 ± 0
HCN + ASA	28 ± 2	–
GSH	10 ± 4	100 ± 0
HCN + GSH	30 ± 3	–

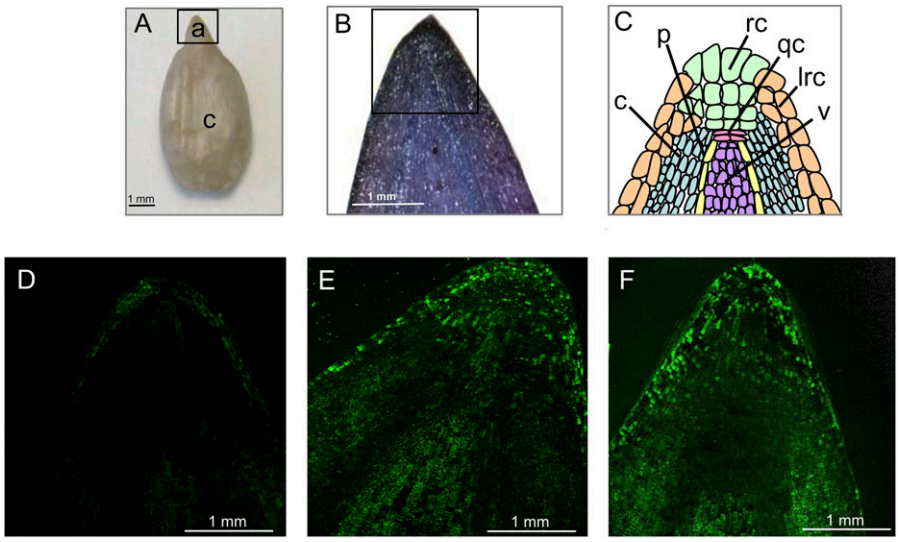

Figure 2. In situ localization of ROS production in the embryonic axes of sunflower embryos. A, Embryo showing axe (a) and cotyledon (c; inset frame corresponds to the view shown in B). B, Staining of embryonic axis by toluidine blue (inset frame corresponds to the views shown in confocal). C, Schematic representation of views shown in D to F. c, Cortex; p, pericycle; rc, root cap; qc, quiescent center; lrc, lateral root cap; v, vascular. D to F, Representative fluorescence images of sections of embryonic axes treated with DCFH-DA viewed by confocal laser scanning microscopy. Axes from dormant embryos imbibed for 24 h on water (D), from nondormant embryos imbibed for 24 h on water (E), and from dormant embryos treated for 3 h with cyanide and further imbibed on water (F; total treatment time was 24 h). Images correspond to maximum projections of Z planes as described in "Materials and Methods." [See online article for color version of this figure.]

The main purpose of this study was nevertheless to determine whether HCN and MV had the same effects on expression of the studied genes, and Figure 3 was designed to directly compare these effects. The value 1 was assigned to the level of gene expression measured in dormant HCN-treated axes. This figure shows that expression of most of the genes studied was similar in the presence of MV and HCN, since it did not vary more than two times when MV was applied instead of HCN, and that the expression of these genes is either inhibited (*HaPOX* and *HaCaM*), stimulated (*HaERF1*), or unchanged (*HaNADPHox*, *HaPOX*, *HaAO1*, *HaAO2*, *HaSer/ThrPK*, *HaMAPK6*, *HaPTP*, *HaETR1*, *HaERS*, and *HaCTR1*) by these compounds (Supplemental Fig. S2). *HaERF1* expression was stimulated by both compounds but more markedly when MV was used instead of HCN. The greatest difference was found for *HaETR2* expression, which was stimulated three times more by MV than HCN (Fig. 3; Supplemental Fig. S2).

DISCUSSION

This article demonstrates that the HCN signal transduction is mediated by ROS and, consequently, that ROS play a key role in the germination process. The first line of evidence supporting this conclusion is brought by the use of ROS or ROS-generating compounds during imbibition of dormant embryos, since

Table III. *Changes in carbohydrate contents in embryonic axes during imbibition*

Carbohydrate content in embryonic axes isolated from dormant sunflower embryos before imbibition (dry), from embryos that were imbibed on water for 3 and 24 h at 10°C (H_2O), and HCN-treated embryos (HCN) imbibed for 3 h in gaseous HCN and then transferred for 21 h on water at 10°C. Values are means of five replicates ± SD. nd, Nondetectable; DW, dry weight.

Treatment	Duration of Imbibition	Carbohydrate Content			
		Suc	Fru	Glc	Raffinose
	h	*μg g DW*$^{-1}$			
No	0 (dry)	17.08 ± 0.50	1.12 ± 0.22	1.86 ± 0.37	8.59 ± 0.88
H_2O	3	12.88 ± 0.34	1.05 ± 0.34	1.74 ± 0.56	8.17 ± 1.13
HCN	3	17.41 ± 1.90	1.42 ± 0.23	2.35 ± 0.38	5.85 ± 0.86
H_2O	24	9.73 ± 0.36	0.49 ± 0.07	0.81 ± 0.12	4.01 ± 0.34
HCN	24	6.96 ± 0.67	nd	nd	4.45 ± 0.79

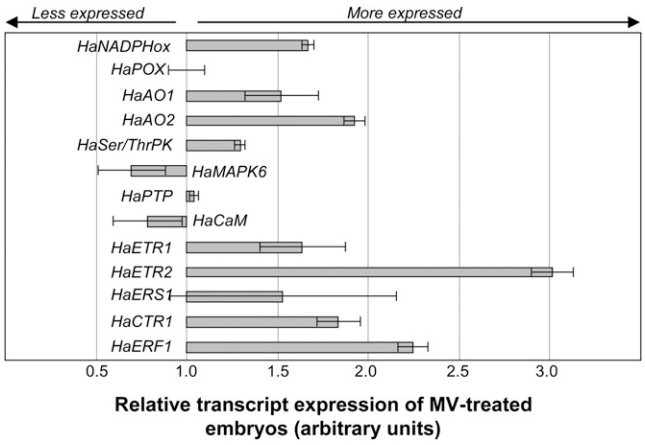

Figure 3. Comparison of the effects of HCN and MV on transcript expression of *HaNADPHox*, *HaPOX*, *HaAO1*, *HaAO2*, *HaSer/ThrPK*, *HaMAPK6*, *HaPTP*, *HaCaM*, *HaETR1*, *HaETR2*, *HaERS1*, *HaCTR1*, and *HaERF1* in embryonic axes isolated from dormant sunflower embryos after 24 h of imbibition at 10°C. Bars denote the relative transcript expression in MV-treated embryos, imbibed for 24 h at 10°C on water, which was calculated as a function of the expression found in HCN-treated embryos to which the value 1 has been assigned. Gaseous HCN and MV (1 mM) were applied during the first 3 h of imbibition. Data were produced using semiquantitative RT-PCR (*HaETR1* and *HaERS1*) and real-time RT-PCR (all other genes) and are means of four biological replicates ± SD.

MV and MN are able to release seed dormancy in a similar manner as observed for HCN (Fig. 1). MV gains electrons from reductants to form the MV cation radical, $MV^{\bullet+}$, which reacts with ground state oxygen to produce $O_2^{\bullet-}$ (Calderbank and Slade, 1976). MN, a precursor of vitamin K_2, is a redox-active quinone that enhances ROS production mainly in mitochondria where it competes with the ubiquinone pool for electrons from complexes I and II (Thor et al., 1982). Both compounds are frequently used to induce oxidative stress. H_2O_2 and the CAT inhibitor AT were less efficient in stimulating germination in dormant embryos (Fig. 1). H_2O_2 is probably rapidly degraded by the various peroxidases in the seed tissues, reducing its effect on germination. Inhibition of CAT by AT was not sufficient to fully release dormancy, which suggests that full dormancy alleviation also requires that ROS-generating processes are activated so that the ROS level is increased to a sufficient level for triggering germination (Bailly et al., 2008). The hypothesis that HCN interacts with ROS-producing pathways is also supported by data on intracellular ROS production in response to HCN treatment. During seed imbibition, nondormant embryonic axes accumulated more ROS than dormant ones (Table I). The nondormant embryos had a very high viability (i.e. almost all tested seeds germinated) and did not accumulate malondialdehyde, an indicator of lipid peroxidation (data not shown), which suggests that the increased ROS production was not deleterious, but more likely, that ROS were involved in cell signaling. HCN treatment of dormant embryos was also associated with an increase in ROS levels, particularly H_2O_2 (Table I). Finally, the last bundle of evidence demonstrating the tight relationship between HCN effect on germination and ROS signaling was brought when using various ROS scavengers since these formers almost fully suppressed the alleviation of embryonic dormancy by HCN (Table II).

ROS imaging with confocal laser scanning microscopy revealed that ROS preferentially accumulated in the radicle tip of germinating embryos in both nondormant, germinating embryos and in embryos whose dormancy was broken after HCN treatment (Fig. 2). The confocal views show that ROS were mainly generated in the root cap and lateral root cap, but they also accumulated in cortex cells. All these cells elongate during the germination process. Production of ROS in the growing part of the radicle might be, at least partly, related to their role in cell elongation. ROS have been shown to be involved in cell expansion during the morphogenesis of organs (Carol and Dolan, 2006). This effect would be related to the effect of ROS on calcium influxes via calcium channels or to their alteration of cell wall properties (Schweikert et al., 2000; Liszkay et al., 2004). As for the effect of HCN described here, the effect of ROS on cell expansion requires NADPH activity (Carol and Dolan, 2006), which suggests that the ROS generated after the HCN treatment could also play a role in cell elongation related to radicle protrusion.

Changes in ROS homeostasis generally result from an alteration in the balance between ROS-producing and -scavenging processes. In agreement with previous works (Grossmann, 2003; Tejera García et al., 2007), we found that KCN was a potent inhibitor of the metalloenzymes CAT and SOD but not of the FAD-containing enzyme GR (Supplemental Fig. S1). The cyanide content of dormant embryonic axes after 3 h of treatment by gaseous HCN was close to 750 μmol g/dry weight (Oracz et al., 2008), a level that is sufficient to inhibit CAT and SOD (Supplemental Fig. S1). The use of DPI, an inhibitor of NADPH oxidase, moreover suggests that HCN effect might involve this enzyme since the treatment by gaseous cyanide was less efficient for releasing dormancy when it was carried out in the presence of DPI (Fig. 1B). It has been suggested that NADPH oxidase plays a role in seed germination in rice (*Oryza sativa*; Liu et al., 2007) and warm-season C4-grasses (Sarath et al., 2007). Consequently, we propose that the increase in cellular ROS content in response to HCN stimulates embryo elongation as a result of the inhibition of ROS-scavenging enzymes, such as CAT and SOD, in conjunction with the stimulation of ROS-generating enzymes, such as NADPHox. Our measurements of soluble sugars (Table III) allowed us to rule out a possible involvement of gluconeogenesis in ROS production after HCN treatment, since seed imbibition leads to the complete use of Glc, which serves as a respiratory substrate. These data are in agreement with the ones published by Walters et al.

(2005), which showed that in sunflower seeds lipid breakdown does not occur before radicle protrusion. Lipid mobilization, leading to subsequent gluconeogenesis, is indeed a significant source of ROS, mainly through the cycle of β-oxidation (Graham, 2008).

Knowing that nonenzymatic mechanisms can also participate to the changes in ROS homeostasis, we also paid attention to the changes in GSH content during embryo dormancy release. Imbibition of HCN-treated dormant embryos shifted the percentage of GSSG toward higher values compared to nondormant embryos (Supplemental Table S1), which is indicative of more oxidizing conditions, in agreement with the ROS measurement data. This very small shift in GSH half-cell reduction potential does not support the hypothesis that changes in GSH/GSSG redox state or GR activity play a major role in HCN-dependent dormancy alleviation. It is important to note that redox changes of high and low molecular weight thiols, such as thioredoxins and GSH, respectively, apparently play a central role in the onset of metabolism during germination (Kranner and Grill, 1993; Buchanan and Balmer, 2005), but a role of thiol-disulphide conversion in dormancy alleviation is not supported by this article.

Increased production of ROS, including H_2O_2 (Caliskan and Cuming, 1998; Schopfer et al., 2001; Bailly et al., 2002; Wojtyla et al., 2006), $O_2^{\bullet -}$ (Gidrol et al., 1994; Liu et al., 2007), and hydroxyl radicals (Schopfer et al., 2001), as well as reactive nitrogen species, such as nitric oxide (Caro and Puntarulo, 1999; Sarath et al., 2007), has been reported for germinating seeds of plant species from different taxonomic backgrounds. Many hypotheses have been put forward for a function of ROS and nitrogen species in the germination process (El-Maarouf-Bouteau and Bailly, 2008). Bailly et al. (2008) proposed that an oxidative window for germination restricts the occurrence of cellular germination-related events to a defined range of ROS level. The data presented here support this hypothesis since low ROS concentrations do not permit germination to progress, potentially due to insufficient signaling. Our data from germinating embryos (i.e. nondormant or dormant embryos treated by HCN or MV) suggest that in sunflower axes this lower limit would be close to 2 nmol g dry weight^{-1} H_2O_2 at the onset of imbibition (Table III). Interestingly, in animal systems, the effects of cyanide on cellular metabolism have also been attributed to ROS generation (Gunasekar et al., 1996; Jones et al., 2003). In plants, this mechanism is now emerging, but it has also to be compared to the effects of sodium nitroprusside (SNP) on germination (Sarath et al., 2006). SNP is widely used as a nitric oxide donor, but it also generates cyanide (Bethke et al., 2005). Therefore, in experimental systems using SNP, cyanide produced is also likely to trigger ROS generation, and the interplay between the various activated oxygen species, such as H_2O_2 and nitric oxide, should be carefully addressed to discriminate

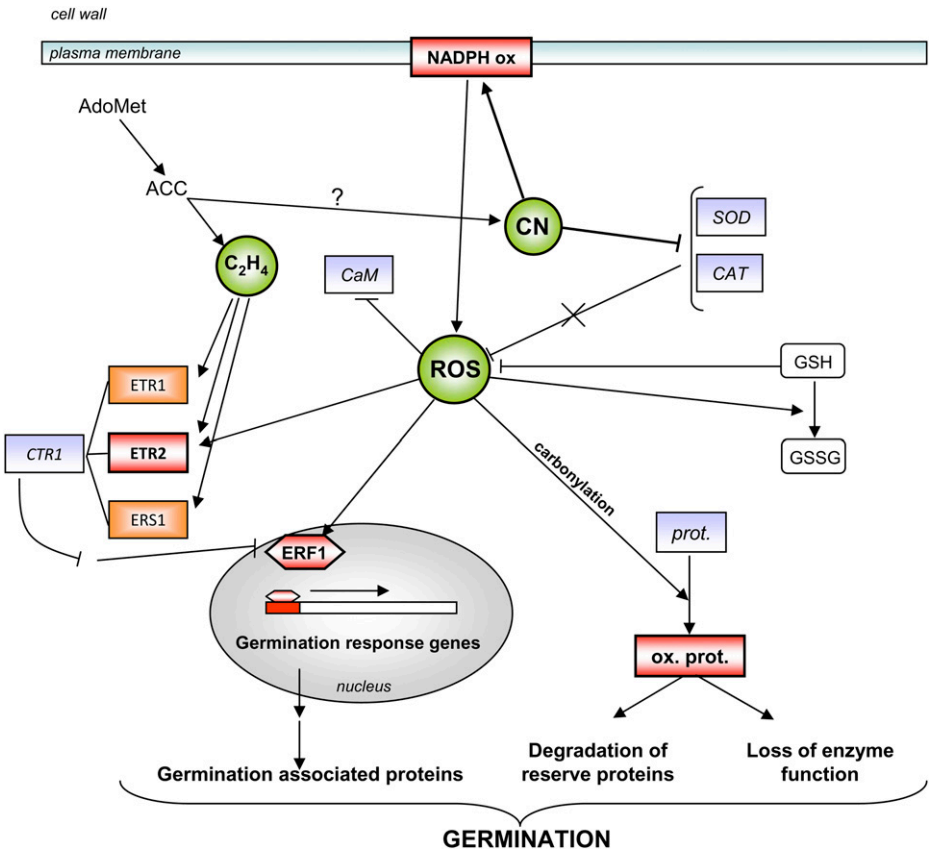

Figure 4. A scheme showing the interactions between HCN (CN in image) and ROS in dormancy alleviation, also integrating data from Oracz et al. (2007, 2008). Positive regulators of dormancy alleviation are written in bold and negative ones in italic. ETR1, ETR2, Ethylene receptor 1 and 2, respectively; ERS1, ethylene response factor 1; CTR1, constitutive triple response 1; ERF1, ethylene response factor 1; AdoMet, *S*-adenosylmethionine; ACC, 1-aminocyclopropane 1-carboxylic acid; prot., protein; ox. prot., oxidized protein. [See online article for color version of this figure.]

between specific and nonspecific effects of these signaling molecules.

Based on the relationship between HCN and ROS metabolism shown previously, we investigated the putative role of HCN on part of the so-called ROS gene network that includes genes involved in ROS production (Mittler et al., 2004), ROS sensing, and transduction. The expression of all studied genes related to ROS production and sensing studied showed a very similar response to both HCN and MV treatment (Fig. 3; Supplemental Fig. S2). The lack of a strong effect of HCN and MV on *HaNADPHox* expression (Supplemental Fig. S2) suggests that NADPH oxidase is probably regulated at the transcriptional and/or posttranscriptional level during dormancy alleviation, since we have shown that NADPHox activity is involved in the ROS generation mediated by HCN (Fig. 1). *HaCaM* expression in dormant embryonic axes was decreased similarly and dramatically in response to HCN and MV treatments (Supplemental Fig. S2), which suggests that the effect of HCN on the expression of this gene might be mediated by ROS. The CaM1 gene was activated synergistically by ABA and H_2O_2 in maize (*Zea mays*) leaves (Hu et al., 2007). Similarly, the stomatal response to ABA involves H_2O_2 and calcium signaling in Arabidopsis (Suhita et al., 2004). Desikan et al. (2001) also showed that CaM was induced by H_2O_2 in cells of Arabidopsis. In contrast, in our investigation, this gene was clearly negatively regulated by HCN and MV, which demonstrates the plasticity of the cellular responses to ROS as a function of the plant organ considered or of its physiological status. For example, the plasticity in the regulation of gene expression by ROS is well illustrated by the cross talk between ABA and H_2O_2. In stomata, ABA and H_2O_2 act synergistically (Wang and Song, 2008) whereas in seeds, where ABA inhibits germination, ABA and H_2O_2 have an antagonistic effect in the control of the germination process (El-Maarouf-Bouteau and Bailly, 2008).

Since it was previously demonstrated that cyanide stimulated the expression of the ethylene response

Table IV. *Main characteristics of genes and primer sequences used in this work*

id, Identity; hom, homology; aa, amino acid; NCBI, National Center for Biotechnology Information.

Name of Sunflower Gene	Putative Function	GenBank of CGP EST Accession No.	Amplification Product Size	Primer Sequences	Identity Percentage of EST Sequences with Other Plants (Plant, Accession No.)	Presence of Conserved Domain (Search against NCBI Conserved Domain Database)
HaNADPHox	NADPHox	>QH_CA_ Contig929	116	Forward: AGGGTCGTTTGACTGGTTC Reverse: ACCGAGCATCACCTTCTTC	79% id bp (*Nicotiana benthamiana*, AB079499)	Oxidoreductase FAD-binding domain
HaPOX	Peroxidase I	>QH_CA_ Contig2935	101	Forward: CCTCCGTTATTCGCCTTC Reverse: ATTGGCTGCTGACTCCTTC	71% hom aa (Arabidopsis, NP_172906)	Plant peroxidase superfamily domain
HaAO1	Amine oxidase	>QHL17I14.yg.ab1	108	Forward: CGACTGTATCATCATCGAGTT Reverse: GCGTTACAAACTGGCAAATC	80% id aa (*Solanum lycopersicum*, CAI39243)	Cu-amine-oxide superfamily domain: copper amine oxidase, catalytic domain
HaAO2	Amine oxidase	>QH_CA_ Contig3110	181	Forward: CGTCCTTTGGTATGTGTTTG Reverse: GGTTTCTTTATGCTCGGTGT	79% id bp (G*lycine max*, AF089851)	No putative domain
HaSer/ThrK	Ser/Thr protein kinase	>QHB16I20.yg.ab1	195	Forward: CAAGGGAGGTGACTTTGG Reverse: ATGTTGGCATACGGCTCT	86% id aa (Arabidopsis, BAF01492)	S_tkc superfamily domain: Ser/Thr protein kinases, catalytic domain
HaMAPK6	Mitogen-activated protein kinase	>QH_CA_ Contig1463	182	Forward: CAAGCAACCCTCTACTGAAC Reverse: GCAACCCACAGACCATAC	87% id aa (*Solanum tuberosum*, BAB93530)	S_tkc superfamily domain
HaCaM	Calmodulin	>QH_CA_ Contig1037	168	Forward: GAGTTCCTTGGTGGTGATG Reverse: GACCTGTGTTGTCGTTTCAG	94% id aa (Arabidopsis, NP_850860)	EF-hand, calcium binding motif
HaPTP	Protein Tyr phosphatase	>QH_CA_ Contig640	107	Forward: TTTCAAGTGGAGGTTGTGGT Reverse: GAGGGAGGATTTGGTGTTG	59% hom aa (Arabidopsis, CAB62119)	No putative domain
Haβ-tubulin	β-Tubulin	QH_CA_Contig4019	132	Forward: GGCGTCTACCTTCATTGGT Reverse: TCCATCTCATCCATTCCTTC	95% hom aa (Arabidopsis, NP_568960)	β-Tubulin domain

factor *HaERF1* (Oracz et al., 2008), we also studied the effect of MV on *HaERF1* but also on four genes involved in ethylene signaling (*HaETR1*, *HaETR2*, *HaERS1*, and *HaCTR1*). The expression of these genes was always higher in the presence of MV than HCN, in particular that of *HaETR2* and *HaERF1* (Fig. 3), which suggests that ROS stimulate some components of the ethylene transduction pathway. ETR2 belongs to the subfamily 2 of membrane-associated receptors (Moussatche and Klee, 2004). In Arabidopsis, Desikan et al. (2005) showed that ETR1, a membrane-associated ethylene receptor of the subfamily 1, was involved in H_2O_2 signaling in guard cells. In sunflower seeds, *HaETR1* was not clearly stimulated by either HCN (Oracz et al., 2008) or MV (Supplemental Fig. S2). As discussed above for the interaction between ABA and H_2O_2, it appears that the regulatory effect of ROS on gene expression may vary in different plant organs. Interestingly, *HaERF1*, a transcription factor in the ERF family (Riechmann et al., 2000), was markedly stimulated by HCN (Oracz et al., 2008) and MV (Fig. 3), which suggests that ERF1 is a common component of HCN, ethylene, and ROS signaling pathways. We propose that the activation of *ERF1* by cyanide is certainly mediated by ROS (Fig. 3). This finding underlines the unique role of ERF in cell signaling since ERFs have been demonstrated to be activated also by jasmonate (Lorenzo et al., 2003) and ABA (Zhang et al., 2004) and to be involved in seed germination (Leubner-Metzger et al., 1998; Song et al., 2005; Pirrello et al., 2006).

In summary, embryo treatment with the ROS-generating MV and treatment with HCN had very similar effects on the regulation of expression of a set of genes. This confirms our previous data obtained using cDNA-amplified fragment length polymorphism, which showed that axes of dormant sunflower seeds treated by either cyanide or MV displayed a majority of identical reproducible transcription-derived fragments (El-Maarouf-Bouteau et al. 2007). These similarities support the view that HCN has not necessarily a direct effect on gene expression, but involves ROS as cellular messengers. The effects of HCN on gene expression are poorly documented in plants and are generally not well understood, probably because HCN targets molecules involved in major metabolic events, such as cytochrome *c* oxidase and hemoproteins. For example, HCN stimulated hemoglobin expression in the aleurone layer of barley (*Hordeum vulgare*) seeds (Nie and Hill, 1997), but this effect was partly attributed to oxygen deprivation. In human cells, HCN can induce oxidative stress and subsequently induce the expression of the nuclear factor κB, a redox-sensitive transcription factor (Shou et al., 2000), and cyclooxygenase-2 (Li et al., 2002).

Together with previously published work (Oracz et al., 2007, 2008) the data presented here provide a comprehensive view of the mechanisms of HCN-dependent dormancy alleviation with ROS as key signaling elements in seed germination. A scheme showing this cross talk is presented in Figure 4. We propose that treatment of sunflower embryos with HCN changes the ROS homeostasis toward higher ROS levels in the embryonic axes, associated with a shift from GSH to GSSG, and which results from the inhibition of antioxidant enzymes, such as CAT and SOD, in conjunction with the stimulation of the ROS-generating enzyme NADPHox. The elevated ROS level can trigger carbonylation of proteins that are specifically associated with seed germination (Oracz et al., 2007). In addition, the transiently increased ROS level can also affect gene expression, in particular that of *CaM*, *ETR2*, and *ERF1*. This suggests that transcriptional and posttranslational events are likely to play a role in the control of seed germination, underlining the high complexity of this process. At last, our set of data emphasizes the role of ROS in cellular signaling during germination and makes them good candidates as key players in the cross talk between hormones that govern dormancy release.

MATERIALS AND METHODS

Plant Material

Sunflower (*Helianthus annuus* 'LG5665') seeds were harvested in 2005 and 2006 near Montélimar (Drôme, France) and purchased from Limagrain. At harvest, dormant seeds were stored at −30°C until use to maintain their dormancy or dry after-ripened at 20°C and 75% relative humidity (i.e. at a moisture content of approximately 0.05 g water/g dry weight) for at least 3 to 4 months to break their dormancy. All the results presented in this study correspond to the means of independent biological replicates obtained with seeds harvested in 2005 and 2006.

Germination Tests

Germination tests were performed with seeds without pericarp (embryos) in darkness, in 9-cm petri dishes (25 seeds per dish and eight replicates) on a layer of cotton wool moistened with deionized water or with various solutions as indicated in the text and at 10°C, a suboptimal temperature for dormant sunflower seed germination (Corbineau et al., 1990). An embryo was considered as germinated when the radicle had elongated to 2 to 3 mm. Germination counts were made daily for 10 d, and the results presented are the means of the germination percentages obtained in eight replicates ± SD as a function of time.

Chemical Treatments

Sunflower seeds were treated with gaseous HCN as described by Bogatek and Lewak (1988). Naked dry embryos were placed in hermetically closed 500-mL flasks on a layer of cotton wool that was moistened with deionized water or with the various chemical compounds mentioned in the text (50 seeds per flask). A glass tube containing 5 mL of 0.1 M KCN placed in the container was used as a source of gaseous HCN, which was produced by acidifying KCN with 5 mL of lactic acid (10%, v/v). In these conditions, the reaction of KCN with lactic acid is very fast and leads to the production of gaseous HCN and K-lactate as a coproduct of the reaction (Bogatek and Lewak, 1988). In a 500-mL jar, the obtained concentration of gaseous HCN is 2.35% (v/v). Such an experimental design allows the seeds to avoid contact with the KCN solution and therefore allows us to rule out any pH effect, and the HCN produced is efficient for releasing seed dormancy without imbibitional water (Oracz et al., 2008). After 3 h of treatment in darkness at 10°C, the flasks were opened and the gaseous cyanide released.

Treatment with MV and MN were carried out by placing embryos on a cotton layer moistened with 0.1 mM MV or 1 mM MN for 3 h.

After treatments, embryos were rinsed carefully three times with deionized water before germination tests or biochemical analyses.

Measurements and in Situ Localization of ROS

Superoxide generation was determined according to the method developed by Elstner and Heupel (1976) based on the oxidation of hydroxylamine to nitrite by $O_2^{\bullet -}$ as previously described (Oracz et al., 2007), using sulfanilamide and 2-naphtylamine. Axes (0.2 g fresh weight) were ground in 4 mL of sodium phosphate buffer (pH 7.8, 50 mM) at 4°C. The extracts were centrifuged at 16,000*g* for 15 min, and the resulting supernatants were used for superoxide determination. The supernatant (1 mL) was first incubated at 25°C for 30 min in the presence of 1 mL hydroxylamine hydrochloride (1 mM) in 50 mM sodium phosphate buffer (pH 7.8). A volume (0.5 mL) of this reaction mixture was then incubated with 0.5 mL of 17 mM sulfanilamide and 0.5 mL of 7 mM 2-naphtylamine at 25°C for 30 min. The absorbance was measured at 540 nm after centrifugation at 13,000*g* for 30 min, and a calibration curve was established using sodium nitrite. The H_2O_2 content of excised axes was determined spectrophotometrically following the protocol described by Oracz et al. (2007) using a peroxidase-based assay with 3-dimethylaminobenzoic acid and 1.3 mM 3-methyl-2-benzothiazolidone hydrazone (O'Kane et al., 1996). In both cases, measurements were carried out with five independent extracts.

ROS production was visualized after ROS staining with DCFH-DA (Schopfer et al., 2001) using confocal laser scanning microscopy. DCFH-DA permeates cells and is hydrolyzed by esterases to liberate DCF, which reacts with H_2O_2 or hydroperoxides to form a fluorescent DCF-derived compound (Sandalio et al., 2008). Thus, the DCFH-DA must not be considered as an indicator of H_2O_2 formation but rather as an indicator of ROS generation (Tarpey et al., 2004). Excised axes were cut longitudinally and incubated in 20 mM potassium phosphate buffer (pH 6.0) containing 100 μM DCFH-DA for 15 min at 10°C. Axes were rinsed for 15 min in the potassium phosphate buffer solution. Images were acquired (excitation, 488 nm; emission, 525 nm) with a Leica SP5 confocal microscope using a ×40/1.25 numerical aperture objective. Z-series were performed with a Z-step of 5 μm, and maximum projections of Z planes are displayed. To compare the intensity of DFCH-DA labeling, axes from different experimental conditions were fixed at the same time and analyzed under the confocal microscope using the same settings. For each axe, a maximal projection of 10 planes was performed, paying attention to start acquisitions at approximately 60 to 80 μm from the cut section to avoid any artefactual signal that may result from wounding.

Axes were also stained for 10 min by 1% (w/v) toluidine blue in 2% (w/v) sodium carbonate to show the organization of the tissue where the confocal sections were taken.

Determination of GSH and GSSG Contents

Extraction and determination of GSH and GSSG in excised axes were carried out according to the method of Kranner and Grill (1996). For each replicate, approximately 25 mg (fresh weigh) of freeze-dried material (five axes) were ground using liquid nitrogen and extracted with 4 mL of 0.1 M HCl on ice. Extracts were centrifuged for 20 min at 20,000*g* at 4°C. Aliquot of the supernatant was used to determine total GSH content (i.e. the sum of GSH + GSSG) and the other for the determination of GSSG after blockage of GSH with *N*-ethylmaleimide (NEM).

For determination of total GSH, 120 μL of the supernatant were mixed with 180 μL of 200 mM 2-(cyclohexylamino)ethanesulfonic acid (CHES) buffer (pH 9.3) and 30 μL of 3 mM dithiothreitol and incubated for 60 min at room temperature to allow reduction of GSSG. The extract was then labeled with 20 μL of monobromobimane for 15 min at room temperature in the dark. The extract was then acidified with 250 μL of 0.25% methanesulfonic acid and centrifuged for 45 min at 20,000*g* at 4°C. The supernatant was used for reversed-phase HPLC (Jasco) analysis. GSH was separated from other low molecular weight thiols on a RP-18 column and detected with a fluorescence detector (excitation, 380 nm; emission, 480 nm). The amounts of GSH in extracts were calculated using a calibration curve (n = four replicates of five axes each).

For determination of GSSG, 400 μL of the supernatant were mixed with 30 μL of 50 mM NEM to block free thiols and 600 μL of 200 mM CHES (pH 9.3) buffer immediately after extraction. After 15 min incubation at room temperature, excess NEM was removed by extracting five times with equal volumes of toluene. Thereafter, 30 μL of 3 mM dithiothreitol were added to a 300-μL aliquot of the NEM treated extract and left for 60 min at room temperature to reduce GSSG. These aliquots were labeled with monobromobimane, acidified with 0.25% methanesulfonic acid, centrifuged and analyzed as described above.

Measurement of Antioxidant Enzyme Activities

Enzyme activities were determined using protein extracts as described by Bailly et al. (1996) using 1 g (fresh weight) of axes. Protein contents in the enzyme extracts were determined using Bio-Rad concentrate dye reagent with bovine serum albumin as a calibration standard. Activity of SOD (EC 1.15.1.1) was determined by measuring the inhibition of nitroblue tetrazolium chloride photoreduction (Giannopolitis and Ries, 1977). SOD activity of is expressed as units SOD mg protein^{-1}. CAT (EC 1.11.1.6) activity was determined according to Bailly et al. (1996). CAT activity is expressed as nmol H_2O_2 decomposed mg protein^{-1} min^{-1}. GR (EC 1.6.4.2) activity was determined following the decrease in absorbance of NADPH at 340 nm (Bailly et al., 1996). GR activity is expressed as nmol NADPH oxidized mg protein^{-1} min^{-1}. For all enzyme activities, three independent replicates were measured.

Sugar Measurements

Soluble sugars were extracted according to Walters et al. (2005). Approximately 40 mg of embryonic axes were ground at room temperature in a mortar in 1 mL 80% aqueous ethanol containing melezitose (2.5 mg mL^{-1}) as internal standard, and the extract was heated for 15 min at 80°C. After centrifugation for 15 min at 14,000*g* and removal of the supernatant, the pellet was resuspended and reextracted in 0.5 mL and then 0.3 mL 80% aqueous ethanol at room temperature and centrifuged again. The supernatants were combined and reduced to dryness in a centrifugal evaporator (RC 10-22; Jouan). The dry extracts were dissolved in 100 μL of ultrapure water and then filtered through acetate filter (0.45-μm pore size; Nalgene) before being analyzed by HPLC. Ten-microliter samples were injected onto a Spherisorb-NH_2 column (Thermo Separation Products) and eluted with 80/20 (v/v) acetonitrile/water at a flow rate of 1 mL min^{-1} using a Spectra Physics 8700 pump. The eluents were analyzed with a differential refractometer (Spectra Physics 8430), and the peak areas were integrated by a Spectra Physics 4290 integrator. Fru, Glc, Suc, and raffinose were identified by coelution with standards (Sigma-Aldrich). The results correspond to the means of five measurements ± SD.

Extraction of Total RNA

Isolated embryonic axes were frozen in liquid nitrogen and stored at −80°C until use. For each extract, 25 axes were ground to a fine powder in liquid nitrogen, and total RNA was extracted by a hot phenol procedure according to Verwoerd et al. (1989). RNA concentration was determined spectrophotometrically at 260 nm.

Primer Design

The oligonucleotide primer sets used for real-time quantitative PCR and semiquantitative reverse transcription (RT)-PCR analysis were designed on the basis of sunflower EST sequences. Candidate sequences were identified in the CGP EST sunflower database (http://cgpdb.ucdavis.edu/) using the BLAST algorithm. The presence of putative domains with sequences corresponding to enzyme functions was highly investigated. Names of used ESTs, homology percentages with other plant sequences, amplified probe length, primer set sequences, and the conserved domains found are listed in Table IV. Gene-specific primers were designed using the Primer3 Input software.

Real-Time Quantitative and Semiquantitative RT-PCR

Total RNA (4 μg) was treated with DNase I (Sigma-Aldrich) and then reverse transcribed with Revertaid H minus M-MuLV RT (Fermentas) for 2 h at 42°C. After enzyme inactivation (10 min at 95°C), the first cDNA strand obtained was checked by 1% agarose gel electrophoresis. Amplification was conducted with real-time PCR (iCycler iQ; Bio-Rad) using 5 μL of 50 times diluted cDNA solution. As an internal standard, a fragment of sunflower *β-tubulin* or *EF1α* gene was used. Real-time PCR reactions were performed with the Absolute qPCR Syber Green Fluorescein mix (Abgene) and 0.25 μM of each primer in a 25-μL reaction volume. Reactions were initiated at 94°C for 15 min followed by 40 cycles at 94°C for 30 s, 56°C for 30 s, and 72°C for 30 s. Calculation of critical threshold (Ct) and relative expressions of genes were performed using the iCycler iQ software (Bio-Rad).

Semiquantitative RT-PCR studies were conducted for *ETR1* and *ERS1* genes. Five microliters of 10 times diluted cDNA reaction mix was used in a

25-μL PCR reaction containing 1.5 mM $MgCl_2$, 10 pM deoxyribonucleotide triphosphate mix, 50 pM of each primer, and 1 unit of Taq polymerase (Invitrogen). The thermocycling conditions were as follows: 5 min at 95°C, 25 cycles of 30 s at 94°C, 30 s at 54°C and 1 min at 72°C, and a final extension of 5 min at 72°C.

Supplemental Data

The following material is available in the online version of this article.

Supplemental Figure S1. Effect of KCN on in vitro activities of catalase, glutathione reductase, and superoxide dismutase extracted from axes isolated from dormant seeds.

Supplemental Figure S2. Expression of *HaNADPHox*, *HaPOX*, *HaAO1*, *HaAO2*, *HaSer/ThrPK*, *HaMAPK6*, *HaPTP*, *HaETR1*, *HaETR2*, *HaERS1*, and *HaERF1* in dormant embryonic axes on water with or without treatment by HCN or MV and in nondormant embryonic axes on water.

Supplemental Table S1. Effect of HCN on GSH and GSSG contents in dormant and nondormant embryonic axes.

ACKNOWLEDGMENT

Confocal imaging was carried out at the IFR83 Cell Imaging Facility, Université Pierre et Marie Curie, Paris.

Received March 4, 2009; accepted March 26, 2009; published March 27, 2009.

LITERATURE CITED

Amory AM, Ford L, Pammenter NW, Cresswell CF (1992) The use of 3-amino-1,2,4-triazole to investigate the short-term effects of oxygen toxicity on carbon assimilation by *Pisum sativum* seedlings. Plant Cell Environ **15:** 655–663

Bailly C, Benamar A, Corbineau F, Côme D (1996) Changes in malondialdehyde content and in superoxide dismutase, catalase and glutathione reductase activities in sunflower seeds as related to deterioration during accelerated aging. Physiol Plant **97:** 104–110

Bailly C, Bogatek-Leszczynska R, Côme D, Corbineau F (2002) Changes in activities of antioxidant enzymes and lipoxygenase during growth of sunflower seedlings from seeds of different vigour. Seed Sci Res **12:** 47–55

Bailly C, El-Maarouf-Bouteau H, Corbineau F (2008) From intracellular signaling networks to cell death: the dual role of reactive oxygen species in seed physiology. C R Biol **331:** 806–814

Berlett BS, Stadtman ER (1997) Protein oxidation in aging, disease and oxidative stress. J Biol Chem **272:** 20313–20316

Bethke PC, Libourel IG, Reinohl V, Jones RL (2005) Sodium nitroprusside, cyanide, nitrite, and nitrate break Arabidopsis seed dormancy in a nitric oxide-dependent manner. Planta **223:** 805–812

Bindschedler LV, Dewdney J, Blee KA, Stone JM, Asai T, Plotnikov J, Denoux C, Hayes T, Gerrish C, Davies DR, et al (2006) Peroxidase-dependent apoplastic oxidative burst in Arabidopsis required for pathogen resistance. Plant J **47:** 851–863

Bogatek R, Lewak S (1988) Effect of cyanide and cold treatment on sugar catabolism in apple seeds during dormancy removal. Physiol Plant **73:** 406–411

Bolwell GP, Wojtaszek P (1997) Mechanisms for the generation of reactive oxygen species in plant defence: a broad perspective. Physiol Mol Plant Pathol **51:** 347–366

Buchanan BB, Balmer Y (2005) Redox regulation: a broadening horizon. Annu Rev Plant Biol **56:** 187–220

Calderbank A, Slade P (1976) Diquat and paraquat. *In* PC Kearney, DD Kaufman, eds, Herbicides, Chemistry Degradation and Mode of Action, Ed 2, Vol 2. Marcel Dekker, New York, pp 501–533

Caliskan M, Cuming AC (1998) Spatial specificity of H_2O_2-generating oxalate oxidase gene expression during wheat embryo germination. Plant J **15:** 165–171

Caro A, Puntarulo S (1999) Nitric oxide generation by soybean embryonic axes. Possible effect on mitochondrial function. Free Radic Res **31:** S205–S212

Côme D, Corbineau F (1990) Some aspects of metabolic regulation of seed germination and dormancy. *In* RB Taylorson, ed, Recent Advances in Development and Germination of Seeds. Plenum Publishing, New York, pp 165–179

Côme D, Corbineau F, Lecat S (1988) Some aspects of metabolic regulation of cereal seed germination and dormancy. Seed Sci Technol **16:** 175–186

Cona A, Rea G, Angelini R, Federico R, Tavladoraki P (2006) Function of amine oxidases in plant development and defence. Trends Plant Sci **11:** 80–88

Carol RJ, Dolan L (2006) The role of reactive oxygen species in cell growth: lessons from root hairs. J Exp Bot **57:** 1829–1834

Corbineau F, Bagniol S, Côme D (1990) Sunflower (*Helianthus annuus*) seed dormancy and its regulation by ethylene. Isr J Bot **39:** 313–325

Desikan R, A-H-Mackerness S, Hancock JT, Neill SJ (2001) Regulation of the Arabidopsis transcriptome by oxidative stress. Plant Physiol **127:** 159–172

Desikan R, Hancock JT, Bright J, Harrison J, Weir I, Hooley R, Neill SJ (2005) A role for ETR1 in hydrogen peroxide signaling in stomatal guard cells. Plant Physiol **137:** 831–834

Dixon DP, Fordham-Skelton AP, Edwards R (2005) Redox regulation of a soybean tyrosine-specific protein phosphatase. Biochemistry **44:** 7696–7703

El-Maarouf-Bouteau H, Bailly C (2008) Oxidative signaling in seed dormancy and germination. Plant Signal Behav **3:** 1–8

El-Maarouf-Bouteau H, Job C, Job D, Corbineau F, Bailly C (2007) ROS signaling in seed dormancy alleviation. Plant Signal Behav **2:** 362–364

Elstner EF, Heupel A (1976) Inhibition of nitrite formation from hydroxylammoniumchloride: a simple assay for superoxide dismutase. Anal Biochem **70:** 616–620

Esashi Y, Ohhara Y, Okazaki M, Hishinuma K (1979) Control of cocklebur seed germination by nitrogenous compounds: nitrite, nitrate, hydroxylamine, thiourea, azide and cyanide. Plant Cell Physiol **20:** 349–361

Finkelstein R, Reeves W, Ariizumi T, Steber C (2008) Molecular aspects of seed dormancy. Annu Rev Plant Biol **59:** 387–415

Foyer CH, Noctor G (2005) Redox homeostasis and antioxidant signaling: a metabolic interface between stress perception and physiological responses. Plant Cell **17:** 1866–1875

Giannopolitis CN, Ries SK (1977) Superoxide dismutases: I. Occurrence in higher plants. Plant Physiol **59:** 309–314

Gidrol X, Lin WS, Degousee N, Yip SF, Kush A (1994) Accumulation of reactive oxygen species and oxidation of cytokinin in germinating soybean seeds. Eur J Biochem **224:** 21–28

Graham IA (2008) Seed storage oil mobilization. Annu Rev Plant Biol **59:** 115–142

Grossmann K (2003) Mediation of herbicide effects by hormone interactions. J Plant Growth Regul **22:** 109–122

Gunasekar PG, Sun PW, Kanthasamy AG, Borowitz JL, Isom GE (1996) Cyanide-induced neurotoxicity involves nitric oxide and reactive oxygen species generation after N-methyl-D-aspartate receptor activation. J Pharmacol Exp Ther **277:** 150–155

Hu X, Jiang M, Zhang J, Zhang A, Lin F, Tan M (2007) Calcium-calmodulin is required for abscisic acid-induced antioxidant defense and functions both upstream and downstream of H_2O_2 production in leaves of maize (*Zea mays*) plants. New Phytol **173:** 27–38

Hung KT, Kao CH (2004) Nitric oxide acts as an antioxidant and delays methyl jasmonate-induced senescence of rice leaves. J Plant Physiol **161:** 43–52

Jonak C, Okrész L, Bögre L, Hirt H (2002) Complexity, cross talk and integration of plant MAP kinase signalling. Curr Opin Plant Biol **5:** 415–424

Jones DC, Prabhakaran K, Li L, Gunasekar PG, Shou Y, Borowitz JL, Isom GE (2003) Cyanide enhancement of dopamine-induced apoptosis in mesencephalic cells involves mitochondrial dysfunction and oxidative stress. Neurotoxicology **24:** 333–342

Kranner I, Birtić S, Anderson KM, Pritchard HW (2006) Glutathione half-cell reduction potential: a universal stress marker and modulator of programmed cell death? Free Radic Biol Med **40:** 2155–2165

Kranner I, Grill D (1993) Content of low-molecular-weight thiols during the imbibition of pea seeds. Physiol Plant **88:** 557–562

Kranner I, Grill D (1996) Determination of glutathione and glutathione disulfide in lichens: a comparison of frequently used methods. Phytochem Anal **7:** 24–28

Kwak JM, Nguyen V, Schoeder JI (2006) The role of reactive oxygen species in hormonal responses. Plant Physiol **141:** 323–329

Lamb C, Dixon RA (1997) The oxidative burst in plant disease resistance. Annu Rev Plant Physiol Plant Mol Biol **48:** 251–275

Laurenzi M, Rea G, Federico R, Tavladoraki P, Angelini R (1999) De-etiolation causes a phytochrome-mediated increase of polyamine oxidase expression in outer tissues of the maize mesocotyl: a role in the photomodulation of growth and cell wall differentiation. Planta **208:** 146–154

Leubner-Metzger G, Petruzzelli L, Waldvogel R, Vögeli-Lange R, Meins F Jr (1998) Ethylene-responsive element binding protein (EREBP) expression and the transcriptional regulation of class I β-1,3-glucanase during tobacco seed germination. Plant Mol Biol **38:** 785–795

Levine A, Tenhaken R, Dixon R, Lamb C (1994) H_2O_2 from the oxidative burst orchestrates the plant hypersensitive disease resistance response. Cell **79:** 583–593

Li L, Prabhakaran K, Shou Y, Borowitz JL, Isom GE (2002) Oxidative stress and cyclooxygenase-2 induction mediate cyanide-induced apoptosis of cortical cells. Toxicol Appl Pharmacol **185:** 55–63

Liszkay A, van der Zalm E, Schopfer P (2004) Production of reactive oxygen intermediates ($O_2^{\bullet-}$, H_2O_2, and $^{\bullet}OH$) by maize roots and their role in wall loosening and elongation growth. Plant Physiol **136:** 3114–3123

Liu X, Xing D, Li L, Zhang L (2007) Rapid determination of seed vigor based on the level of superoxide generation during early imbibition. Photochem Photobiol Sci **6:** 767–774

Lorenzo O, Piqueras R, Sánchez-Serrano JJ, Solano R (2003) ETHYLENE RESPONSE FACTOR1 integrates signals from ethylene and jasmonate pathways in plant defense. Plant Cell **15:** 165–178

Miller G, Shulaev V, Mittler R (2008) Reactive oxygen signaling and abiotic stress. Physiol Plant **133:** 481–489

Mittler R, Vanderauwera S, Gollery M, Van Breusegem F (2004) Reactive oxygen gene network of plants. Trends Plant Sci **9:** 490–498

Moussatche P, Klee HJ (2004) Autophosphorylation activity of the Arabidopsis ethylene receptor multigene family. J Biol Chem **279:** 48734–48741

Nie X, Hill RD (1997) Mitochondrial respiration and hemoglobin gene expression in barley aleurone tissue. Plant Physiol **114:** 835–840

Noctor G, Foyer CH (1998) Ascorbate and glutathione: keeping active oxygen under control. Annu Rev Plant Physiol Plant Mol Biol **49:** 249–279

O'Kane D, Gill V, Boyd P, Burdon R (1996) Chilling, oxidative stress and antioxidant responses in *Arabidopsis thaliana* callus. Planta **198:** 371–377

Oracz K, El-Maarouf-Bouteau H, Bogatek R, Corbineau F, Bailly C (2008) Release of sunflower seed dormancy by cyanide: cross-talk with ethylene signalling pathway. J Exp Bot **59:** 2241–2251

Oracz K, El-Maarouf Bouteau H, Farrant JM, Cooper K, Belghazi M, Job C, Job D, Corbineau F, Bailly C (2007) ROS production and protein oxidation as a novel mechanism for seed dormancy alleviation. Plant J **50:** 452–465

Pirrello J, Jaimes-Miranda F, Sanchez-Ballesta MT, Tournier B, Khalil-Ahmad Q, Regad F, Latché A, Pech JC, Bouzayen M (2006) Sl-ERF2, a tomato ethylene response factor involved in ethylene response and seed germination. Plant Cell Physiol **47:** 1195–1205

Quettier AL, Bertrand C, Habricot Y, Miginiac E, Agnes C, Jeannette E, Maldiney R (2006) The phs1-3 mutation in a putative dual-specificity protein tyrosine phosphatase gene provokes hypersensitive responses to abscisic acid in *Arabidopsis thaliana*. Plant J **47:** 711–719

Rea G, De Pinto MC, Tavazza R, Biondi S, Gobbi V, Ferrante P, De Gara L, Federico R, Angelini R, Tavladoraki P (2004) Ectopic expression of maize polyamine oxidase and pea copper amine oxidase in the cell wall of tobacco plants. Plant Physiol **134:** 1414–1426

Rentel MC, Lecourieux D, Ouaked F, Usher SL, Petersen L, Okamoto H, Knight H, Peck SC, Grierson CS, Hirt H, et al (2004) OXI1 kinase is necessary for oxidative burst-mediated signaling in Arabidopsis. Nature **427:** 858–861

Riechmann JL, Heard J, Martin G, Reuber L, Jiang C, Keddie J, Adam L, Pineda O, Ratcliffe OJ, Samaha RR, et al (2000) *Arabidopsis* transcription factors: genome-wide comparative analysis among eukaryotes. Science **290:** 2105–2110

Roberts EH (1973) Oxidative processes and the control of seed germination. *In* W Heydecker, ed, Seed Ecology. Butterworths, London, pp 189–218

Roberts EH, Smith RD (1977) Dormancy and the pentose phosphate pathway. *In* AA Khan, ed, The Physiology and Biochemistry of Seed Dormancy and Germination. Elsevier North-Holland Biomedical Press, Amsterdam, pp 385–411

Sandalio LM, Rodriguez-Serrano M, Romero-Puertas MC, Del Rio LA (2008) Imaging of reactive oxygen species and nitric oxide *in vivo* in plant tissues. Methods Enzymol **440:** 397–409

Sarath G, Bethke PC, Jones R, Baird LM, Hou G, Mitchell RB (2006) Nitric oxide accelerates seed germination in warm-season grasses. Planta **223:** 1154–1164

Sarath G, Hou G, Baird LM, Mitchell RB (2007) Reactive oxygen species, ABA and nitric oxide interactions on the germination of warm-season C (4)-grasses. Planta **226:** 697–708

Schopfer P, Plachy C, Frahry G (2001) Release of reactive oxygen intermediates (superoxide radicals, hydrogen peroxide, and hydroxyl radicals) and peroxidase in germinating radish seeds controlled by light, gibberellin, and abscisic acid. Plant Physiol **125:** 1591–1602

Schweikert C, Liszkay A, Schopfer P (2000) Scission of polysaccharides by peroxidase-generated hydroxyl radicals. Phytochemistry **53:** 565–570

Shou Y, Gunasekar PG, Borowitz JL, Isom GE (2000) Cyanide-induced apoptosis involves oxidative-stress-activated NF-kappaB in cortical neurons. Toxicol Appl Pharmacol **164:** 196–205

Song CP, Agarwal M, Ohta M, Guo Y, Halfter U, Wang P, Zhu JK (2005) Role of an *Arabidopsis* AP2/EREBP-type transcriptional repressor in abscisic acid and drought stress responses. Plant Cell **17:** 2384–2396

Suhita D, Raghavendra AS, Kwak JM, Vavasseur A (2004) Cytoplasmic alkalization precedes reactive oxygen species production during methyl jasmonate- and abscisic acid-induced stomatal closure. Plant Physiol **134:** 1536–1545

Tarpey MM, Wink DA, Grisham MB (2004) Methods for detection of reactive metabolites of oxygen and nitrogen: *in vitro* and *in vivo* considerations. Am J Physiol Regul Integr Comp Physiol **286:** R431–R444

Tejera García NA, Iribarne C, Palma F, Lluch C (2007) Inhibition of the catalase activity from *Phaseolus vulgaris* and *Medicago sativa* by sodium chloride. Plant Physiol Biochem **45:** 535–541

Thor H, Smith MT, Hartzell P, Bellomo G, Jewell SA, Orrenius S (1982) The metabolism of menadione (2-methyl-1,4-naphthoquinone) by isolated hepatocytes: a study of the implications of oxidative stress in intact cells. J Biol Chem **257:** 12419–12425

Verwoerd TC, Dekker BMM, Hoekema A (1989) A small-scale procedure for the rapid isolation of plant RNAs. Nucleic Acids Res **17:** 2362

Walters C, Landré P, Hill L, Corbineau F, Bailly C (2005) Organization of lipid reserves in cotyledons of primed and aged sunflower seeds. Planta **222:** 397–407

Wang PT, Song CP (2008) Guard-cell signalling for hydrogen peroxide and abscisic acid. New Phytol **178:** 703–718

Wise RR, Naylor AW (1987) Chilling-enhanced photo-oxidation: evidence for the role singlet oxygen and endogenous antioxidants. Plant Physiol **83:** 278–282

Wojtyla L, Garnczarska M, Zalewski T, Bednarski W, Ratajczak L, Jurga S (2006) A comparative study of water distribution, free radical production and activation of antioxidative metabolism in germinating pea seeds. J Plant Physiol **163:** 1207–1220

Xing Y, Jia W, Zhang J (2008) AtMKK1 mediates ABA-induced CAT1 expression and H_2O_2 production via AtMPK6-coupled signaling in Arabidopsis. Plant J **54:** 440–451

Zhang H, Huang Z, Xie B, Chen Q, Tian X, Zhang X, Zhang H, Lu X, Huang D, Huang R (2004) The ethylene-, jasmonate-, abscisic acid- and NaCl-responsive tomato transcription factor JERF1 modulates expression of GCC box-containing genes and salt tolerance in tobacco. Planta **220:** 262–270